THE JOURNAL OF BIOLOGICAL CHEMISTRY VOL. 285, NO. 17, pp. 12735–12746, April 23, 2010

Identification of *Conus* Peptidylprolyl Cis-Trans Isomerases (PPIases) and Assessment of Their Role in the Oxidative Folding of Conotoxins[S]

Received for publication, October 25, 2009, and in revised form, February 9, 2010 Published, JBC Papers in Press, February 10, 2010, DOI 10.1074/jbc.M109.078691

Helena Safavi-Hemami[‡], Grzegorz Bulaj[§], Baldomero M. Olivera[¶], Nicholas A. Williamson[‡], and Anthony W. Purcell[‡1]

From the [‡]Department of Biochemistry and Molecular Biology, The Bio21 Molecular Science and Biotechnology Institute, University of Melbourne, 3010 Victoria, Australia and the Departments of [§]Medicinal Chemistry and [¶]Biology, University of Utah, Salt Lake City, Utah 84108

Peptidylprolyl cis-trans isomerases (PPIases) are ubiquitous proteins that catalyze the cis-trans isomerization of prolines. A number of proteins, such as *Drosophila* rhodopsin and the human immunodeficiency viral protein HIV-1 Gag, have been identified as endogenous substrates for PPIases. However, very little is known about the interaction of PPIases with small, disulfide-rich peptides. Marine cone snails synthesize a wide array of cysteine-rich peptides, called conotoxins, many of which contain one or more prolines or hydroxyprolines. To identify whether PPIase-associated cis-trans isomerization of these residues affects the oxidative folding of conotoxins, we identified, sequenced, and expressed three functionally active isoforms of PPIase from the venom gland of *Conus novaehollandiae*, and we characterized their ability to facilitate oxidative folding of conotoxins *in vitro*. Three conotoxins, namely μ-GIIIA, μ-SIIIA, and ω-MVIIC, derived from two distinct toxin gene families were assayed. *Conus* PPIase significantly increased the rate of appearance of the native form of μ-GIIIA, a peptide containing three hydroxyprolines. In contrast, the presence of PPIase had no effect on the folding of μ-SIIIA and ω-MVIIC, peptides containing no or one proline residue, respectively. We further showed that an endoplasmic reticulum-resident PPIase isoform facilitated folding of μ-GIIIA more efficiently than two cytosolic isoforms. This is the first study to demonstrate PPIase-assisted folding of conotoxins, small disulfide-rich peptides with unique structural properties.

Predatory marine cone snails (genus *Conus*) synthesize a great diversity (>50,000) of neurotoxic peptides commonly referred to as conotoxins. Conotoxins selectively target specific subtypes of receptors or ion channels throughout the nervous system, a characteristic that has lead to wide use of conotoxins in ion channel research and as therapeutic agents (for review see Refs.1 and 2). It is now well understood that the vast diversity of conotoxins is driven by two major events: gene duplication followed by hypermutation of the mature toxin region (3) and the generation of posttranslational modifications (for review see Ref. 4). Posttranslational modifications in *Conus* generally aid in stabilizing the peptide structure (5, 6) as well as varying the structure and shape of the peptide to optimize target binding (7–9).

The most common posttranslational modification is the formation of disulfide bonds, a characteristic shared with neurotoxins from other venomous animals, antimicrobial peptides such as the defensins, and peptide proteinase inhibitors (Table 1). Conotoxins can be grouped into several superfamilies on the basis of their N-terminal signal sequence and their conserved disulfide framework. Interestingly, despite thousands of different toxin sequences biosynthesized there are only 12–18 structural scaffolds found *in vivo*, an obscurity recently referred to as the "conotoxin folding puzzle" (10). Even within the same disulfide scaffold, various conotoxins display an array of folding properties, suggesting that neither the Cys pattern nor the primary amino acid sequence is a key folding determinant *in vitro* (10). Discrepancies between *in vivo* and *in vitro* folding of conotoxins are emerging (10), with toxins that are difficult to synthesize chemically often being highly abundant in the snail venom gland (11, 12). These findings strongly suggest that the three-dimensional structure that conotoxins adopt *in vivo* is determined by specific interactions with folding enzymes and molecular chaperones. One apparent folding catalyst in the biosynthesis of cysteine-rich peptides is protein-disulfide isomerase (PDI).[2] The oxidation and isomerization of disulfide bonds in the ER of *Conus* are now known to be catalyzed by PDI (13), one of the most abundant soluble proteins in the venom gland of *Conus* (14, 15). Given the structural complexity of conotoxins, mechanisms other than PDI-mediated folding are likely to occur.

A great number of conotoxins comprise one or more proline (Pro) residues, some of which are important for toxin-target interactions (16, 17). Hydroxylation of these Pro residues is a common modification in *Conus* and has recently been reported to affect the oxidative folding properties of several conotoxins including ω-MVIIC, a toxin with very poor *in vitro* folding

[S] The on-line version of this article (available at http://www.jbc.org) contains supplemental Figs. 1 and 2 and Table 1.

The nucleotide sequence(s) reported in this paper has been submitted to the GenBank™/EBI Data Bank with accession number(s) GU046310–GU046313 and GU067468.

[1] To whom correspondence should be addressed. Tel.: 613-8344-2288; Fax: 613-9348-1421; E-mail: apurcell@unimelb.edu.au.

[2] The abbreviations used are: PDI, protein-disulfide isomerase; CHAPS, 3-[(3-cholamidopropyl)dimethylammonio]-1-propanesulfonic acid; Cyp, cyclophilin; ER, endoplasmic reticulum; HPLC, high pressure liquid chromatography; IEF, isoelectric focusing; LC, liquid chromatography; MALDI-TOF, matrix-assisted laser desorption ionization time-of-flight; MS/MS, tandem mass spectroscopy; *p*NA, *p*-nitroanilide; PPIase, peptidylprolyl cis-trans isomerase; RACE, rapid amplification of cDNA ends; RT, reverse transcriptase; Suc, succinyl.

yields (18). Hydroxylation of Pro leads to a 2-fold increase in folding yields, whereas the neurotoxic activity of the toxin is maintained. For the μ-conotoxin GIIIA, the modification enhances bioactivity but does not affect folding. In contrast, Pro hydroxylation impairs activity but improves folding yields in the two α-conotoxins ImI and GI, which naturally contain a conserved Pro residue (18). These findings emphasize the importance of Pro hydroxylation in the structure and bioactivity of conotoxins. Hydroxylation of Pro has been reported for a number of proteins including collagen, a well studied substrate of the enzyme peptidylprolyl cis-trans isomerase (PPIase) (19–21).

PPIases are ubiquitous enzymes found in vertebrates, invertebrates, plants, and bacteria and are present in almost all cellular compartments (for review see Ref. 22). Today the terms PPIases, cyclophilins (Cyp), and immunophilins are often used synonymously. Genome analysis of the yeast *Saccharomyces cerevisiae* identified at least eight different isoforms (23), none of which are essential for its survival (24). The human genome comprises at least 16 genes encoding for Cyp-like proteins, eight of which have been identified in *vivo* (for review see Ref. 22). Many functions have been described for these diverse proteins including roles in cellular signaling (25) and the regulation of gene transcription (26, 27) and as chaperones and folding catalysts (28–30). Mammalian CypA is located in the cytosol where it is known to bind the immunosuppressive drug cyclosporine (31). Formation of the CypA-cyclosporine complex prevents T-cell proliferation via inhibition of the protein phosphatase calcineurin (32, 33). The two PPIase isoforms CypB and FKBP-13 reside in the ER (34, 35) and are overexpressed during heat shock, suggesting a major role in the folding and/or assembly of proteins (36, 37). Peptidylprolyl bonds can adopt two distinct conformations, cis or trans. PPIases catalyze the cis-trans isomerization of these bonds, an otherwise slow process that can impede protein folding. A number of proteins have been identified as *in vivo* (30, 38) and *in vitro* (19, 39) folding substrates for PPIases; however, little is known about their role in the folding of small cysteine-rich peptides. In the only study reported to date, the effects of the human cytosolic PPIase FKBP-12 on the oxidative folding of the scorpion toxin maurotoxin were evaluated (for sequence see Table 1) (40). The presence of PPIase accelerated the disappearance of intermediate folding species but does not change the overall folding kinetics of maurotoxin *in vitro* (40).

To address the paucity of information on conotoxin biosynthesis, the present study aimed to identify enzymes having the potential to assist conotoxin folding *in vivo*. We hypothesized that given the frequency of peptidylprolyl bonds in conotoxins and their importance for receptor binding, PPIase-mediated cis-trans isomerization of these bonds facilitates oxidative folding during toxin biosynthesis in the ER of *Conus*. To test this hypothesis we first identified and sequenced several PPIase isoforms in the venom gland of the Australian cone snail, *Conus novaehollandiae*, and recombinantly expressed functionally active enzymes. We demonstrate that PPIase-mediated isomerization of peptidylprolyl bonds significantly affects the rate of formation of the native disulfide bonds for the μ-conotoxin GIIIA, a peptide with three hydroxyprolines (Hyp) and three disulfide bonds. We further show that an ER-resident PPIase is more active in accelerating the folding of μ-GIIIA when compared with two cytosolic isoforms. This study furthers our knowledge on how cone snails efficiently synthesize such a great diversity of highly structured peptides and may shed light on the fundamental principals of oxidative folding of small cysteine-rich peptides.

EXPERIMENTAL PROCEDURES

Specimen Collection, Tissue Preparation, and Histology—Live specimens of *C. novaehollandiae* (Adams, 1854) were collected from Broome, Western Australia. For protein and RNA extractions, venom glands, venom bulbs, and muscle tissues were dissected, immediately snap-frozen in liquid nitrogen, and stored at −80 °C until further processing. For histological preparations, adult snails were transferred to seawater containing 2% $MgCl_2$ for 4 h. The shells were cracked, the viscera were removed, and overnight fixation was performed in 4% paraformaldehyde/phosphate-buffered saline. Fixed specimens were processed, sectioned (7 μm), and stained with Mallory's trichrome stain (41) following routine histological procedures.

Protein Extraction and Two-dimensional Gel Electrophoresis—Frozen venom ducts were pooled (a total of two samples pooled from three snails each), ground under liquid nitrogen, resuspended in 1 ml of cell lysis buffer (10 mM Tris-HCl, 100 mM NaCl, 1 mM EDTA, 1 mM NaF, 20 mM $Na_4P_2O_7$, 1% Triton-X, 10% glycerol, 0.1% SDS, 1 mM phenylmethylsulfonyl fluoride, 1× Complete protease inhibitor mixture (Roche Applied Science), pH 7.6), and incubated for 30 min on ice. Cell lysates were centrifuged, and proteins were precipitated from the supernatants and reconstituted in rehydration buffer (8 M urea, 2% CHAPS, 0.002% bromphenol blue, 20 mM dithiothreitol, 0.5% immobilized pH gradient buffer, pH 3–11 (GE Healthcare)) at a final concentration of 1 mg/ml in preparation for isoelectric focusing (IEF). Protein precipitation (2-D Clean-Up Kit, GE Healthcare) and quantitation (BCA assay kit, Thermo Fisher Scientific) were performed according to the manufacturer's instructions. Two hundred μg of protein was applied onto a nonlinear, pH 3–11, immobilized pH gradient strip (Immobiline, GE Healthcare) and rehydrated overnight. IEF was performed on the Ettan IPGphor II IEF system (GE Healthcare). Running conditions were 500 V for 1 h at 0.5 kVh, 1000 V for 1 h at 0.8 kVh, 6000 V for 2 h at 7.0 kVh, and 6000 V for 40 min at 0.7–3.7 kVh. Following IEF, strips were reduced in equilibration buffer (75 mM Tris-HCl, 6 M urea, 30% glycerol, 2% SDS, 0.002% bromphenol blue) containing 65 mM dithiothreitol for 15 min followed by alkylation for 15 min in the presence of 80 mM iodoacetamide. Second dimension gel electrophoreses were performed on 8–16% Tris-HCl SDS-PAGE (Criterion, Bio-Rad) for 50 min at 200 V. Gels were stained with Coomassie Brilliant Blue G-250 (Bio-Rad). In-gel digestion and protein identification were performed as described previously (42). Briefly, two-dimensional gel electrophoresis spots were excised, washed in 50% acetonitrile/triethylammonium bicarbonate, and reduced with 20 mM dithiothreitol followed by alkylation in 100 mM iodoacetamide. In-gel digestion was performed using sequencing grade trypsin (Sigma-Aldrich) at a final concentration of 10 μg/ml in 25 mM triethylammonium

TABLE 1
Diversity of proline/hydroxyproline-containing disulfide-rich peptides
*, C-terminal amidation; O, hydroxyproline; γ, γ-carboxylation of glutamate. Prolines/hydroxyprolines are highlighted gray, and cysteine residues are shown in bold.

Peptide	Sequence / disulfide pattern	Species, common name	Function
conotoxin GS	ACSGRGSRCOOQCC MGLRCGRGNPQKC	*Conus geographus*, geography cone	Na^+ channel inhibitor
attracotoxin	LLACLFGNGRCSSNRDCCELTPVCKRGSCVSSGPGLVG	*Hadronyche infensa*, funnel web spider	Na^+ channel inhibitor
α-conotoxin GI	ECCNPACGRHYSC*	*Conus geographus*, geography cone	nAChR inhibitor
κM-conotoxin RIIIK	LOSCCSLNLRLCOVOACKRNOCCT*	*Conus radiatus*, rayed cone	K^+ channel inhibitor
Apamin	CNCKAPETALCARRCQQH*	*Apis mellifera*, honey bee	K^+ channel inhibitor
Maurotoxin	VSCTGSKDCYAPCRKQTGCPNAKCINKSCKCYGC*	*Scorpio maurus palmatus*, chactoid scorpion	K^+ channel blocker
PTU1 toxin	AEKDCIAPGAPCFGTDKPCCNPRAWCSSYANKCL	*Peirates turpis*, assasin bug	Ca^{2+} channel inhibitor
Huwentoxin-X	KCLPPGKPCYGATQKPCCGVCSHNKCT	*Ornithoctonus huwena*, chinese earth tiger	Ca^{2+} channel inhibitor
Katala B1	CGETCVGGTCNTPGCTCSWPVCTRNGLPV	*Oldenlandia affinis*	plant defense
Leginsulin	ADCNGACSPFEVPPCRSRDCRCVPIGLFVGFCIHPTG	*Glycine max*, soybean	plant hormone
Guanylin	PGTCEICAYAACTGC	*Homo sapiens*, human	Intestinal hormone
Defensin Hbd-2	PVTCLKSGAICHPVFCPRRYKQIGTCGLPGTKCCKKP	*Homo sapiens*, human	antimicrobial activity
Bv-IWF4	SGECNMYGRCPPGYCCSKFGYCGVGRAYCG	*Eucommia ulmoides*, hardy rubber tree	antimicrobial activity
EAFP1	QTCASRCPRPCNAGLCCSIYGYCGSGNAYCGAGNCRCQCRG	*Allomyrina dichotoma*, Japanese rhinoceros beetle	antimicrobial activity
EETHI	GCPRILMRCKQDSDCLAGCVCGPNGFCGSP	*Ecballium elaterium*, squirting cucumber	trypsin inhibitor
MCPI IIa	HADPICNKPCKTHDDCSGAWFCQACWNSARTCGPYVG	*Solanum tuberosum*, potato	carboxypeptidase inhibitor
AAI	CIPKWNRCGPKMDGVPCCEPYTCTSDYYGNCS	*Amaranthus hypochondriacus*, amaranth plant	alpha-amylase inhibitor
Obtustatin	CTTGPCCRQCKLKPAGTTCWKTSLTSHYCTGKSCDCPLYPG	*Vipendae lebetina obtusa*, blunt-nosed viper	integrin inhibitor
Gurmarin	QQCVKKDELCIPYYLDCCEPLECKKVNWWDHKCIG	*Gymnema sylvestre*, periploca of the woods	supresses sweetness response

bicarbonate. Peptides extracted after overnight digestion were separated on a C18 column (Zorbax 80SB-C18, 74 μm × 43 mm, Agilent, Forest Hill, Victoria, Australia) and analyzed using a linear ion trap mass spectrometer (LC/MSD Trap XCT Plus, Agilent). MS/MS data were used to search the UniProt nonredundant protein data base using Mascot, version 2.2 (Matrix Science, Boston) with the following settings: trypsin, one missed cleavage, carbamidomethyl as a fixed and oxidation of methionine as a variable modification, 1.2 Da peptide tolerance, 0.8 Da MS/MS tolerance, with error-tolerant search included.

cDNA Isolation and Identification of Conus PPIase Transcripts—Three frozen venom ducts were pooled and ground under liquid nitrogen. Total RNA was extracted using TRIzol reagent (Invitrogen). Total RNA was treated with Turbo DNase (Ambion, Scoresby, Victoria, Australia). RNA concentrations

were determined using a spectrophotometer, and RNA integrity was verified by agarose-gel electrophoresis. For rapid amplification of cDNA ends (RACE), 5′ and 3′ universal primer-adapted cDNA was prepared from 1000 ng of total RNA using the SMART™ RACE cDNA amplification kit (Clontech Laboratories, Mountain View, CA). RACE was performed using primary and nested PCR proprietary universal oligonucleotides and three gene-specific oligonucleotides (supplemental Table 1) designed on the basis of conserved gene regions and/or on peptide matches obtained using two-dimensional gel electrophoresis coupled with LC/MS/MS (see above). Primary PCR reactions were performed in volumes of 50 μl containing 2.5 μl of 1:10 diluted cDNA, 0.5 μl of TITANIUM *Taq* DNA polymerase (Clontech), 1× Advantage 2 PCR buffer (Clontech), dNTPs at 200 μM, 5 μl of 10× universal primer A mix (Clontech), and a gene-specific oligonucleotide (0.2 μM) (supplemental Table 1). If the PCR reaction did not produce a visible PCR amplicon, a nested PCR using 5 μl of the primary PCR reaction was performed. To sequence the PPIase A-like isoforms, PCR was performed using redundant oligonucleotides designed to amplify the open reading frame specifically (supplemental Table 1). All PCR amplicons were analyzed by gel electrophoresis, cloned into pGEM-T plasmid vectors (Promega), and subsequently sequenced. Nucleotide sequencing was performed using the ABI Prism BigDye Terminator (version 3.1) cycle sequencing kit (ABI) with the SP6 promoter oligonucleotide (Promega). Samples were analyzed on an ABI 3730xl DNA analyzer (Applied Biosystems). All sequences analyzed in this study were deposited in GenBank™ (National Center for Biotechnology Information, U. S. National Library of Medicine, Bethesda, MD) with the accession numbers shown in supplemental Table 1. All nucleotide data were translated into the predicted amino acid sequences, and comparative alignment of the protein sequences were performed using MAFFT E-INS-i sequence alignment by means of local pairwise alignment information (43).The putative signal peptides were predicted using SignalP software (44).

Reverse Transcription (RT)-PCR—Total RNA was prepared as described above. cDNA was reverse-transcribed from 720 ng of DNase-treated total RNA extracted from venom glands, bulbs, and muscle (total of two samples/tissue, pooled from three snails each) using the Transcriptor High Fidelity cDNA Synthesis Kit (Roche Applied Science). Primary RT-PCR reactions were performed in volumes of 30 μl containing 2 μl of cDNA (60 ng), 0.3 μl of TITANIUM *Taq* DNA polymerase (Clontech), 1× Advantage 2 PCR buffer (Clontech), dNTPs at 200 μM, and 0.2 μM forward and reverse oligonucleotides (supplemental Table 1). To rule out false amplification of genomic DNA, a negative control was performed using the reaction from which the enzyme reverse transcriptase was excluded. To ensure linearity of the reaction and rule out PCR inhibition, RT-PCR on all oligonucleotides and tissues was performed with different concentrations of template cDNA (0.6, 6, 60, and 600 ng) for 25, 30, and 35 amplification cycles (data not shown). All PCR amplicons were analyzed by gel electrophoresis and subsequently sequenced as described above.

Cloning, Expression, and Purification of PPIase Isoforms—Full-length PPI A (isomers I and II) and PPI B lacking the N-terminal signal sequence were cloned into the pET22b+ expression vector containing a C-terminal His_6 tag (Novagen, Kilsyth, Victoria, Australia). Transcripts were PCR-amplified from venom gland cDNA prepared as described above (see supplemental Table 1 for oligonucleotide sequences used). PCR amplicons were ligated into pET22b+ using the BamHI (5′) and XhoI (3′) restriction sites (New England Biolabs, Arundel, Queensland, Australia), and sequences were verified as described above. Constructs were transformed into the Rosetta strain of *Escherichia coli* (Novagen). For expression of *Conus* PPIases, Luria broth medium (Sigma-Aldrich) containing ampicillin (100 μg/ml) and tetracycline (12.5 μg/ml) was inoculated with overnight cultures and incubated at 37 °C with shaking until the A_{600} spectrophotometric reading was 0.6. After the addition of Isopropyl-β-D-thiogalactopyranoside (final concentration 0.1 mM) the bacterial culture was further incubated for 3 h at 25 °C with shaking. Bacteria were harvested and resuspended in native lysis buffer (50 mM NaH_2PO_4, 300 mM NaCl, 10 mM imidazole (Sigma-Aldrich), pH 8.0) containing protease inhibitors (Complete protease inhibitor mixture, Roche Applied Science). Bacterial cells were lysed by incubating them with lysozyme (1 mg/ml, Sigma-Aldrich) on ice for 30 min followed by probe tip sonication. Cellular debris and insoluble protein were pelleted by centrifugation, and the supernatants were used for subsequent protein purifications.

Recombinant *Conus* PPIases were purified on a 1-ml immobilized metal affinity column under native conditions (Bio-Scale Mini Profinity IMAC cartridge, Bio-Rad). Protein purification was performed using the Bio-Rad Profinia protein purification system. Briefly, protein lysates were loaded onto the column at 0.5 ml/min, and nonspecifically bound proteins were removed with native buffer (NB: 300 mM KCl, 50 mM KH_2PO_4, pH 8.0) containing 5 mM imidazole at 2 ml/min for 6 min followed by a second wash with NB containing 10 mM imidazole for 3 min. His-tagged proteins were eluted with 250 mM imidazole in NB at 2 ml/min for 2 min. Further purification and buffer exchange into 0.1 M Tris-HCl, pH 8.0, containing 150 mM NaCl was accomplished by size exclusion chromatography (Superdex 200, HiLoad 16/60, GE Healthcare). Protein concentrations were determined spectrophotometrically using the molar absorption coefficients of the proteins (45). The purified recombinant proteins were analyzed by SDS-PAGE and sequence-verified by in-gel digestion and analysis of proteotypic tryptic peptides as described above.

Protease-coupled PPIase Assay—PPIase activity of recombinant proteins was determined using the coupled chymotrypsin assay (46) with modifications. Briefly, PPI (final concentrations 30 nM for PPI A (I) and (II) and 300 nM for PPI B) was added to 0.1 M Tris-HCl, pH 8, in the absence and presence of a 10× excess of the inhibitor cyclosporine (final concentrations 90 nM for PPI A (I) and (II) and 900 nM for PPI B (Sigma-Aldrich, stock made in ethanol)). After incubation at 25 °C for 2 min, reactions were transferred to 10 °C for 5 min before the addition of 30 μl of 0.6 M chymotrypsin (Sigma-Aldrich). After 5 min at 10 °C, the reaction was initialized with the substrate succinyl-Ala-Ala-Pro-Phe-*p*-nitroanilide (Suc-AAPF-*p*NA) at a final concentration of 78 μM (Bachem AG, Bubendorf, Switzerland; stock made in trifluoroethanol in the presence of 0.45 M LiCl (Sigma-

TABLE 2
Conotoxins used in this study
The letter O in the peptide sequence represents hydroxyproline, and Z stands for pyroglutamic acid. #, denotes a C-terminal amidation; bold letters are conserved cysteines.

Species	Toxin	Sequence	Disulfide scaffold
Conus geographus	GIIIA	RDCCTOOKKCKDRQCKOQRCCA#	μ-conotoxin
Conus striatus	SIIIA	ZNCCNGGCSSKWCRDHARCC#	
Conus magus	MVIIC	CKGKGAPCRKTMYDCCSGSCGRRGKC#	ω-conotoxin
	MVIIC O7P	CKGKGAOCRKTMYDCCSGSCGRRGKC#	

Aldrich)). The cis-trans isomerization was measured by following the absorbance at 390 nM in a Lambda 2 spectrophotometer (PerkinElmer Life Sciences). The mean and standard errors were calculated from three independent experiments.

Peptide Synthesis and Folding—Three conotoxins, μ-GIIIA, μ-SIIIA, and ω-MVIIC, derived from two distinct toxin gene families were selected for oxidative folding studies (Table 2). For MVIIC two analogues were synthesized, containing either a proline (MVIIC) or a hydroxyproline (MVIIC OP7) in position 7. All peptides were produced as described previously (47). Briefly, peptides were synthesized on a solid support by an automated peptide synthesizer using Fmoc (*N*-(9-fluorenyl)methoxycarbonyl) protected amino acids, HBTU (*O*-(benzotriazol-1-yl)-1,1,3,3-tetramethyluronium hexafluorophosphate), and diisopropylethylamine (48). Peptides were cleaved from the resin by treatment with reagent K (trifluoroacetic acid/thioanisole/ethanedithiol/water/phenol (90/5/5/2.5/7.5 by volume)) for 4–4.5 h. The peptides were subsequently filtered, precipitated, and washed with cold methyl *tert*-butyl ether. Linear peptides were purified by reversed-phase HPLC on a semipreparative C18 column (Vydac, 5 μm particle size, 10 × 250 mm; Grace, Deerfield, IL) using a linear gradient from 5 to 40% buffer B (90% acetonitrile, 0.1% trifluoroacetic acid) over 20 min. Absorbance was monitored at 220 nm. Concentrations of SIIIA and MVIIC were determined spectrophotometrically using the molar absorption coefficient of the peptides at 280 nm. The concentration of GIIIA was determined by HPLC. Oxidative folding reactions were carried out in 0.1 M Tris-HCl, pH 7.5, 1 mM EDTA, 0.1 mM reduced glutathione (GSH), and 0.1 mM oxidized glutathione (GSSG) in the presence and absence of PPIase. Folding was initiated by adding the linear peptide at a final concentration of 20 μM. Aliquots were taken at various time points, and reactions were quenched by acidification with formic acid at a final concentration of 8%. Folding reactions were analyzed by reversed-phase HPLC on a C18 column (Vydac, 5 μm particle size, 4.6 × 250 mm; Grace) under the conditions described above. Native peptides were distinguished from linear peptides and other forms on the basis of characteristic HPLC elution profiles (18, 47), mass spectrometric analyses of manually collected reversed-phase fractions (MALDI-TOF mass spectrometer, Ultraflex II in positive reflector mode, Bruker Daltonics, Bremen, Germany), and for the GIIIA experiments coelution with chemically synthesized biologically active GIIIA (18) (supplemental Figs. 1 and 2).

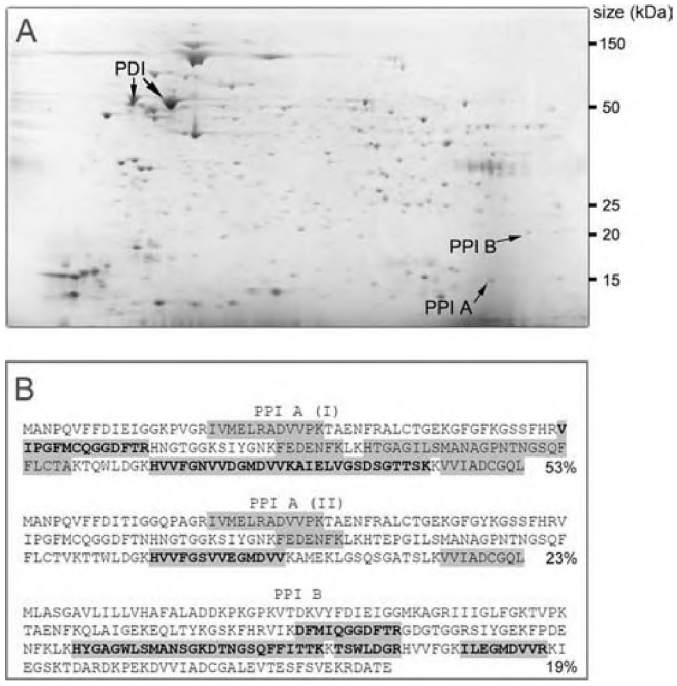

FIGURE 1. **Proteomic identification of *Conus* PPIases.** *A*, two-dimensional gel electrophoresis image of proteins extracted from the venom gland of *C. novaehollandiae* showing proteins subsequently identified as PDI, PPI A, and PPI B. 200 μg of total protein was loaded onto nonlinear pH 3–11 IEF strips and separated on 8–16% Tris-HCl SDS-PAGE. Gel spots were excised, reduced, and alkylated, and trypsin was digested and analyzed by ESI-ion trap LC/MS/MS. Mass spectrometry results were searched against the UniProt protein data base using Mascot software. *B*, protein sequences of *Conus* PPI A (I), A (II), and B obtained by cDNA sequencing. Peptide matches generated by the data base search of the trypsin-digested gel spots are highlighted in *gray* (Mowse score > 54). Unique peptide matches are depicted in *bold*. The percentage of sequence coverage is shown.

RESULTS

Identification of Conus PPI Isoforms Using a Combination of Two-dimensional Gel Electrophoresis and cDNA Sequencing—Two-dimensional gel electrophoresis on venom gland proteins led to the identification of at least three different isoforms of PPIase excised from two distinct gel spots (Fig. 1*A*). Data base searches revealed sequence similarities to cyclophilin A from a number of different species including the German cockroach (GenBank™ accession number CAA60869) and the medicinal leech (GenBank™ accession number AAB01531) and to cyclophilin B from the channel catfish (GenBank™ accession number ABC75555) and the yellow fever mosquito (GenBank™ accession number ABF18081). A number of unique peptides derived from two proteins were identified for one gel spot indicating co-migration of two cyclophilin A isoforms, whereas the other gel spot contained one protein similar to cyclophilin B only. Using this unique sequence information, conventional RT-PCR, and RACE-PCR, a total of four PPIase isoforms were sequenced eventually (Fig. 2). Two cDNA transcripts showed high sequence similarities to cyclophilin A (PPI A) from a range of different organisms such as the Japanese scallop *Chlamys farreri* (identity, 81%; GenBank™ accession number AAR11779.1) and are hereafter referred to as *Conus* PPI A (I) and *Conus* PPI A (II). The A isoform of PPIase is located in the cytosol (49). The two transcripts have open reading frames of 495 bases encoding proteins with a predicted molecular mass of

17,523 and 17,542 Da. A third isoform with sequence identities of 73% to PPI B from *Xenopus laevis* (GenBank™ accession number AAH54168) and 72% to PPI B from *Homo sapiens* (GenBank™ accession number NP_000933) has an open reading frame of 621 bases encoding a protein with a predicted molecular mass of 22,614 Da. An N-terminal cleavage site between alanine 18 and aspartate 19 would release a mature peptide with an expected molecular mass of 20,821 Da as predicted by SignalP software (version 3.0). The presence of an N-terminal signal peptide and its homology to other B isoforms known to be located in the ER (Fig. 3) (49) strongly suggest that the mature protein resides in the ER. Thus, this isoform is hereafter referred to as *Conus* PPI B. The fourth cDNA transcript shares homology with peptidylprolyl isomerase-like 1 protein from a variety of organisms such as the copepod *Caligus rogercresseyi* (similarity, 78%; GenBank™ accession number ACO11158) and *Mus musculus* (similarity,74%; GenBank™ accession number BAE33862). The molecular mass of the predicted protein is 18,560 Da encoded by an open reading frame of 507 bases. This isoform was designated *Conus* PPI C. Protein sequence alignment by means of local pairwise alignment (43) reveals high conservation of the key residues involved in substrate binding between the four isoforms (Fig. 2) (50, 51), the only exception being the presence of serine 103 in PPI B and C instead of the conserved alanine 103 present in both PPI A isoforms. Re-evaluation of the two-dimensional gel electrophoresis data using the protein sequences predicted from the cDNA transcripts shows unique peptide matches and good sequence coverage for the two A isoforms, (I) and (II), co-migrating in one gel spot and PPI B (Fig. 1*B*). Two-dimensional gel electrophoresis further confirmed the presence of two isoforms of *Conus* PDI with high sequence similarities to PDI from *Conus marmoreus* (13) (GenBank™ accession number ABF48564).

Reverse Transcription-PCR of Folding Enzymes across Different Tissue Types—Conotoxins are synthesized in the epithelial cells of the long, tubular venom gland. In contrast, the venom bulb, a muscular organ located at the distal end of the venom gland, has been suggested to be involved in venom translocation rather than venom synthesis (52), whereas the muscle is simply involved in the locomotion of the snail. To assess the potential role of *Conus* PPIases in the folding of conotoxins, differential expression of the newly identified isoforms was determined for these three tissue types using RT-PCR. Although PPI A and PPI C were ubiquitously expressed across the tissue types tested, the ER-resident isoform B exhibited high mRNA expression in the venom gland alongside high expression levels of conotoxins for this organ (Fig. 4).

Expression Purification and Characterization of Conus PPIase Isoforms—On the basis of its potential role in conotoxin folding, the putative mature ER-resident isoform PPI B was expressed in *E. coli*. The two cytosolic "A" isoforms also identified using both two-dimensional electrophoresis and cDNA sequencing were expressed for comparative studies. Purification of the soluble His-tagged fusion proteins using immobilized metal affinity and size exclusion chromatography yielded recombinant proteins of high purity (Fig. 5). The identities of all recombinant proteins were confirmed by nucleotide sequencing and LC/MS/MS analyses of the in-gel-digested SDS-polyacrylamide gel bands (data not shown). To ensure the functionality of the recombinant PPI proteins, their prolyl cis-trans isomerase activity was tested using a modification of the coupled chymotrypsin assay

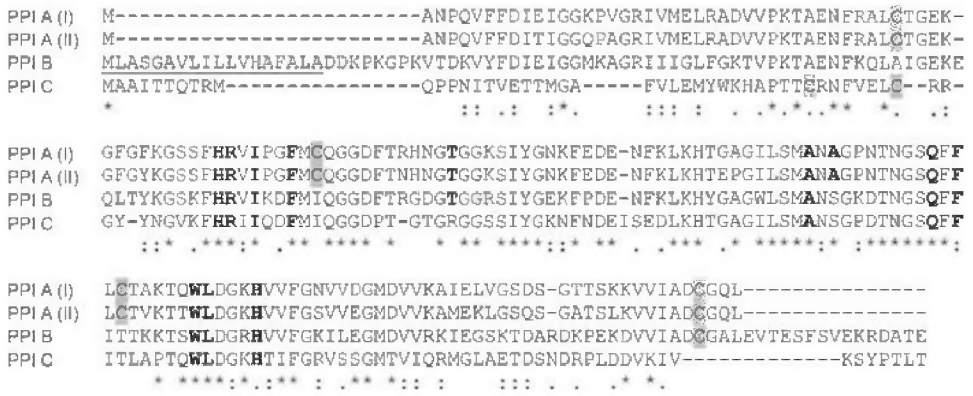

FIGURE 2. **Comparative alignment of PPIases identified in the venom gland of *C. novaehollandiae* (GenBank™ accession numbers: PPI A (I), GU046310; PPI A (II), GU046311; PPI B, GU046312; PPI C, GU046313).** Alignment was performed using MAFFT E-INS-i by means of local pairwise alignment information (43). Side chains forming the binding cleft are shown in *bold* (51). Cysteine residues are *shaded*. The predicted signal sequence of PPI B is *underlined* (SignalP). *Dashes* denote gaps. Amino acid conservations are denoted by *asterisks*, whereas *colons* and *periods* represent a high and low degree of similarity, respectively.

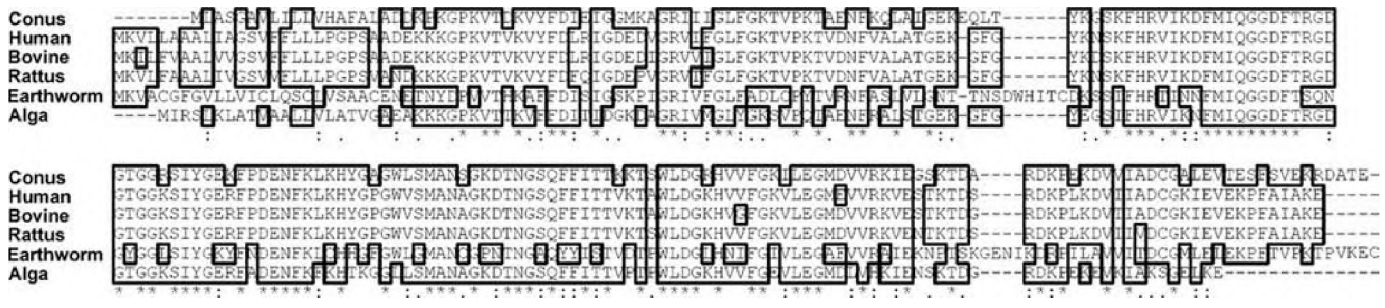

FIGURE 3. **Comparative alignment of the ER-resident B isoform of PPIases.** Alignment was performed using MAFFT E-INS-i by means of local pairwise alignment information (43). Identical amino acids are outlined in *black*. *Dashes* denote gaps. Amino acid conservations are denoted by *asterisks*, whereas *colons* and *periods* represent a high and low degree of similarity, respectively.

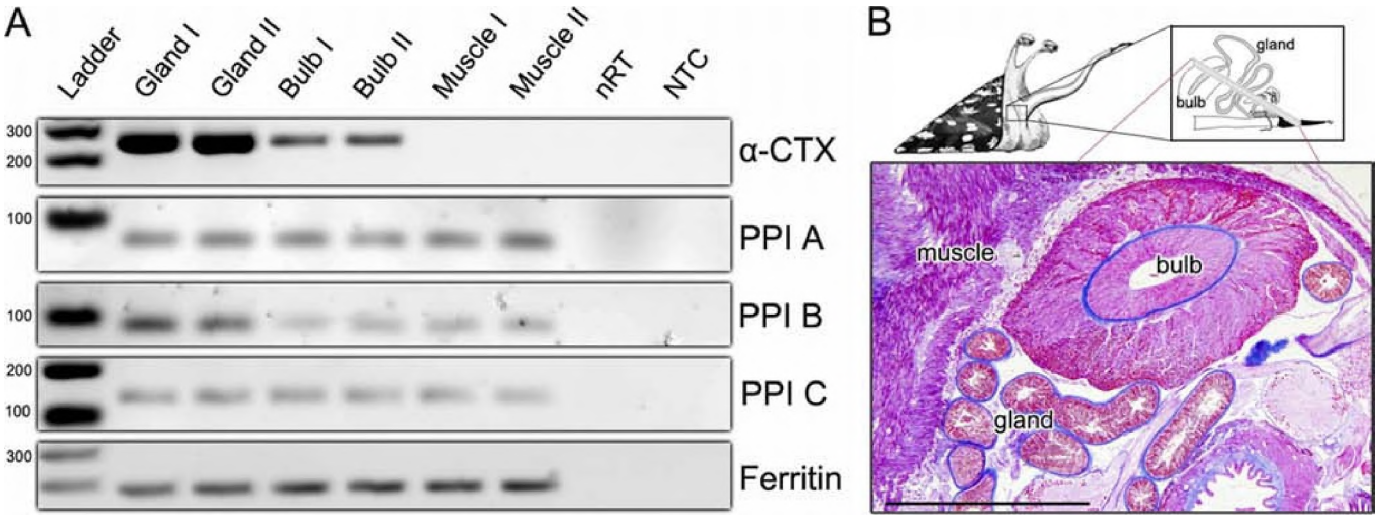

FIGURE 4. **Differential expression of *Conus* PPIases and α-conotoxins across three different tissue types: the venom gland, the venom bulb, and the muscle tissue.** *A*, RT-PCR showing high mRNA expression levels of the ER-resident folding enzyme PPI B in the venom gland when compared with the bulb and muscle tissue. PPI A and PPI C are constitutively expressed across the different tissue types. Ferritin was used as a reference gene. *nRT*, no reverse transcriptase control; *NTC*, no template control. *B*, schematic of cone snail and venom apparatus depicting orientation of histological section and histology showing the tissue used for RT-PCR, a 7-μm section (*scale bar*: 500 μm) stained with Mallory's trichrome stain.

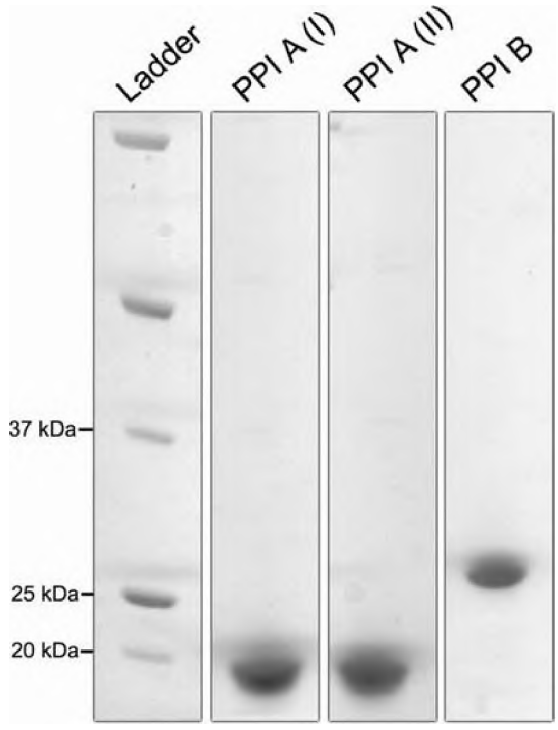

FIGURE 5. **Expressed and purified PPIases cloned from the venom gland of *C. novaehollandiae*.** C-terminal His-tagged fusion proteins were expressed in *E. coli* (Rosetta strain) and purified using immobilized metal affinity chromatography (IMAC) on the Profinia purification system (Bio-Rad) followed by size exclusion chromatography (Superdex 200, GE Healthcare). 1 μg of protein was loaded per lane. *Ladder*, unstained protein ladder (Invitrogen).

(46). All three enzymes exhibited peptidylprolyl isomerase activity that was reduced by preincubation of the reaction with the PPI inhibitor cyclosporine (Fig. 6). Interestingly, the two A isoforms were more active in catalyzing the prolyl cis-trans isomerization of the tetrapeptide Suc-Ala-Ala-Pro-Phe-*p*NA, and higher concentrations of PPI B (300 *versus* 30 nM for PPI A (I) and (II)) had to be used to obtain similar prolyl cis-trans conversion rates.

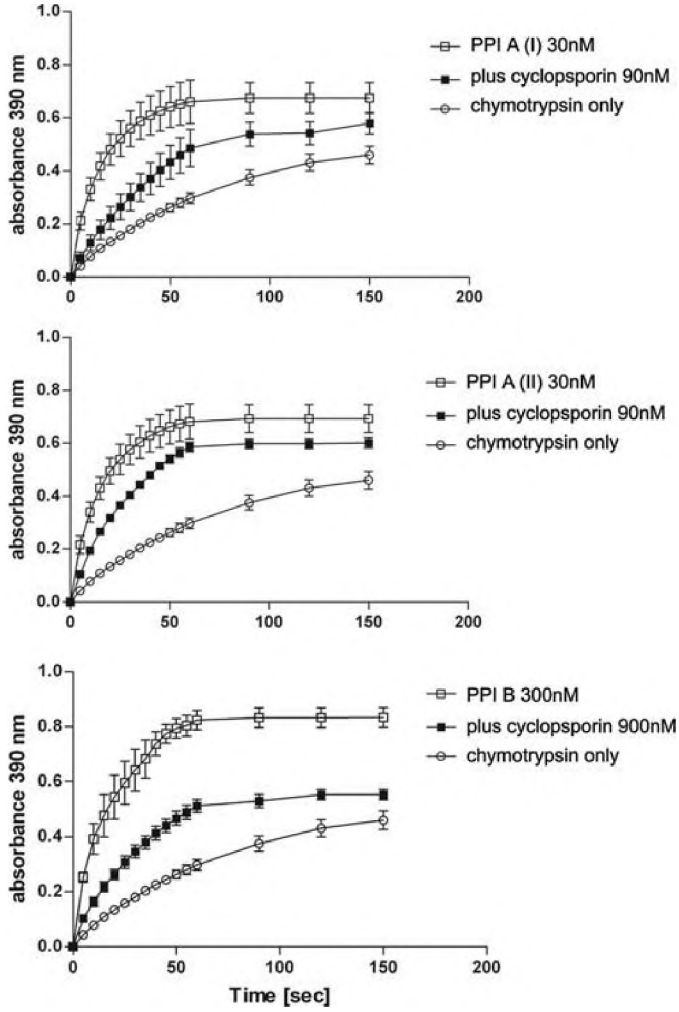

FIGURE 6. **Peptidylprolyl cis-trans isomerase activity of *Conus* PPIase isoforms.** Enzyme activity was tested using the coupled chymotrypsin assay with 30 nM PPI A (I) and (II) and 300 nM PPI B in the presence and absence of the PPIase inhibitor cyclosporine. Reactions containing chymotrypsin only served as base-line controls. Means ± S.E. were calculated from three independent experiments.

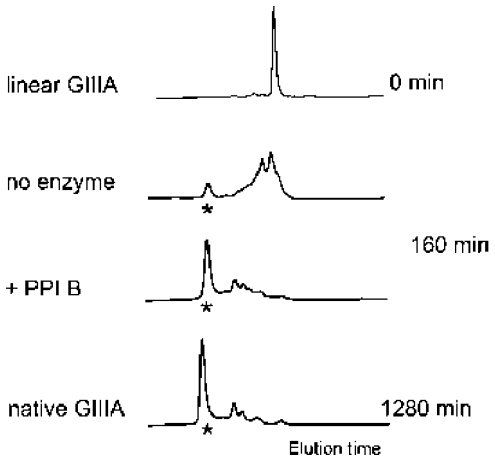

FIGURE 7. **HPLC analysis of the oxidative folding of conotoxin μ-GIIIA carried out in the presence of 0.1 mM GSH and 0.1 mM GSSG with and without *Conus* PPI B.** Folding reactions were quenched at 0 (linear), 160, and 1280 min (native) and analyzed by reversed-phase HPLC (C18 column, Vydac-Grace). *Asterisks* denote the folded species containing the native disulfide connectivity as determined by its characteristic elution profile (18) and coelution studies with biologically active GIIIA (supplemental Fig. 1).

Conotoxin Folding Studies—To investigate the role of *Conus* PPIases in the folding of Pro- and Hyp-containing conotoxins, three conotoxins, namely μ-GIIIA, μ-SIIIA, and ω-MVIIC, were assayed. All three peptides had been studied previously in detail with respect to their oxidative folding properties (18, 53). GIIIA is 22 amino acids in length with a C-terminal amidation and six cysteines forming three disulfide bonds. The mature peptide contains three Hyp residues at position 6, 7, and 17 (Table 2). NMR studies on GIIIA and its paralogue, GIIIB, strongly suggest a trans configuration of Hyp^{6} and Hyp^{17}, whereas Hyp^{7} adopts a cis conformation (54, 55). The other μ-conotoxin tested, SIIIA, is 20 amino acids in length and is C-terminally amidated with the first amino acid being a pyroglutamic acid. SIIIA shares its characteristic disulfide pattern with GIIIA but does not contain proline nor hydroxyproline residues. The ω-conotoxin MVIIC is 26 amino acids in length, C-terminally amidated, and contains six cysteine residues forming three disulfide bonds (Table 2). MVIIC, which contains one proline residue in position 7, is likely to adopt both cis and trans conformations (18). However, as the peptide sequence was originally deduced from cDNA sequence information, hydroxylation of this proline residue may occur *in vivo*. Thus, both the proline (MVIIC)- and hydroxyproline (MVIIC 7PO)-containing peptides were synthesized and tested.

All reversed-phase elution profiles of oxidative folding reactions concurred with those reported previously (Fig. 7) (18, 47). The molecular masses of the collected peaks agreed with the calculated masses as determined by MALDI-TOF mass spectrometric analysis. Oxidative folding of μ-GIIIA was carried out in 0.1 M Tris-HCl, pH 7.5, 1 mM EDTA, 0.1 mM GSH, and 0.1 mM GSSG at room temperature. Under these conditions steady state accumulation of the native peptide occurred after approximately 20 h (Fig. 8*A*) with a half-time of 583 min (471–766 min) (Fig. 8*D* and Table 3). As the PPIase concentration in the ER was not known, enzyme:substrate ratios concurrent with previous studies were used (40, 56). In the presence of 0.5 μM *Conus* PPI B folding was accelerated ~6-fold with a half-time of 100 min (77–141 min) (Fig. 8*D* and Table 3). PPI B did not affect the final folding yields of the native species (51–52%, Table 3). The disappearance of the linear form was accelerated 3.8-fold (Fig. 8, *B* and *D*). Both the initial appearance and the subsequent disappearance of other folding intermediates occurred faster in the presence of PPI B (Fig. 8*C*). Mass spectrometric analysis of the other minor refolded species revealed partial oxidation of cysteine residues, glutathione adducts, and proline cis-trans isomers (supplemental Fig. 2). Enzyme activity was abolished when PPIase was heat-treated for 20 min at 95 °C prior to doing the folding assays (data not shown). Enzyme-assisted folding of GIIIA followed in a concentration-dependent manner (Fig. 9). At a concentration of 25 nM, PPI B showed little improvement in folding kinetics; however, when the enzyme concentration was increased to 2.5 μM, an exponential accumulation of the native peptide was observed (R-value, 0.97; half-time, 61 min (50–78 min) (Fig. 9*A*)). In contrast, PPI B did not accelerate the oxidative folding of SIIIA, MVIIC, and MVIIC P7O under various conditions tested (data not shown). To examine the potential differences between PPI B and the two cytosolic isoforms PPI A (I) and (II), oxidative folding of GIIIA was carried out in the presence of 2.5 μM PPI A (I) and (II), respectively. Interestingly, both PPI A isoforms were less capable of accelerating the folding of GIIIA than PPI B (Fig. 10*A*) with half-times for the appearance of the native peptide of 220 min (156–375 min) for PPI A (I) and 244 min (173–414 min) for PPI A (II) at final concentrations of 2.5 μM enzyme (Fig. 10*B* and Table 3). Because of the nature of the folding assay, constraints with enzyme and substrate concentrations did not allow for the formal measurement of kinetic parameters such as K_m and k_{cat} values.

DISCUSSION

Combining proteomics with targeted cDNA sequencing proved to be a highly successful technique for the discovery of novel proteins in the venom gland of *Conus*. Sequence information obtained by two-dimensional gel electrophoresis and nucleotide sequencing was used for the functional characterization of a group of molecular chaperones, the peptidylprolyl cis-trans isomerases. This study describes for the first time the presence of multiple PPIase isoforms in the venom gland of *Conus* and evaluates PPIase-assisted oxidative folding of conotoxins *in vitro*. Further investigations using this integrated approach of proteomic and molecular analyses will facilitate the identification and characterization of additional venom gland proteins and provide insight into the generation of chemical diversity in *Conus*.

Despite their complex three-dimensional structure, which often comprises multiple disulfide bonds and posttranslational modifications (overview in Refs. 4 and 57), little is known about *in vivo* folding events in the ER of *Conus*. To date, the only ER-resident enzymes identified in *Conus* are γ-carboxylase (58) and PDI (14, 15). PDI was shown to be one of the major soluble proteins in the venom gland of *Conus textile* (14) and *Conus amadis* (15), and oxidative folding studies show PDI-assisted folding of a number of conotoxins *in vitro* including μ-GIIIA (13, 47, 59). Two-dimensional gel electrophoresis analysis of the venom gland proteome confirmed high abundances of this enzyme in the venom gland of *C. novaehollandiae* (Fig. 1*A*). As

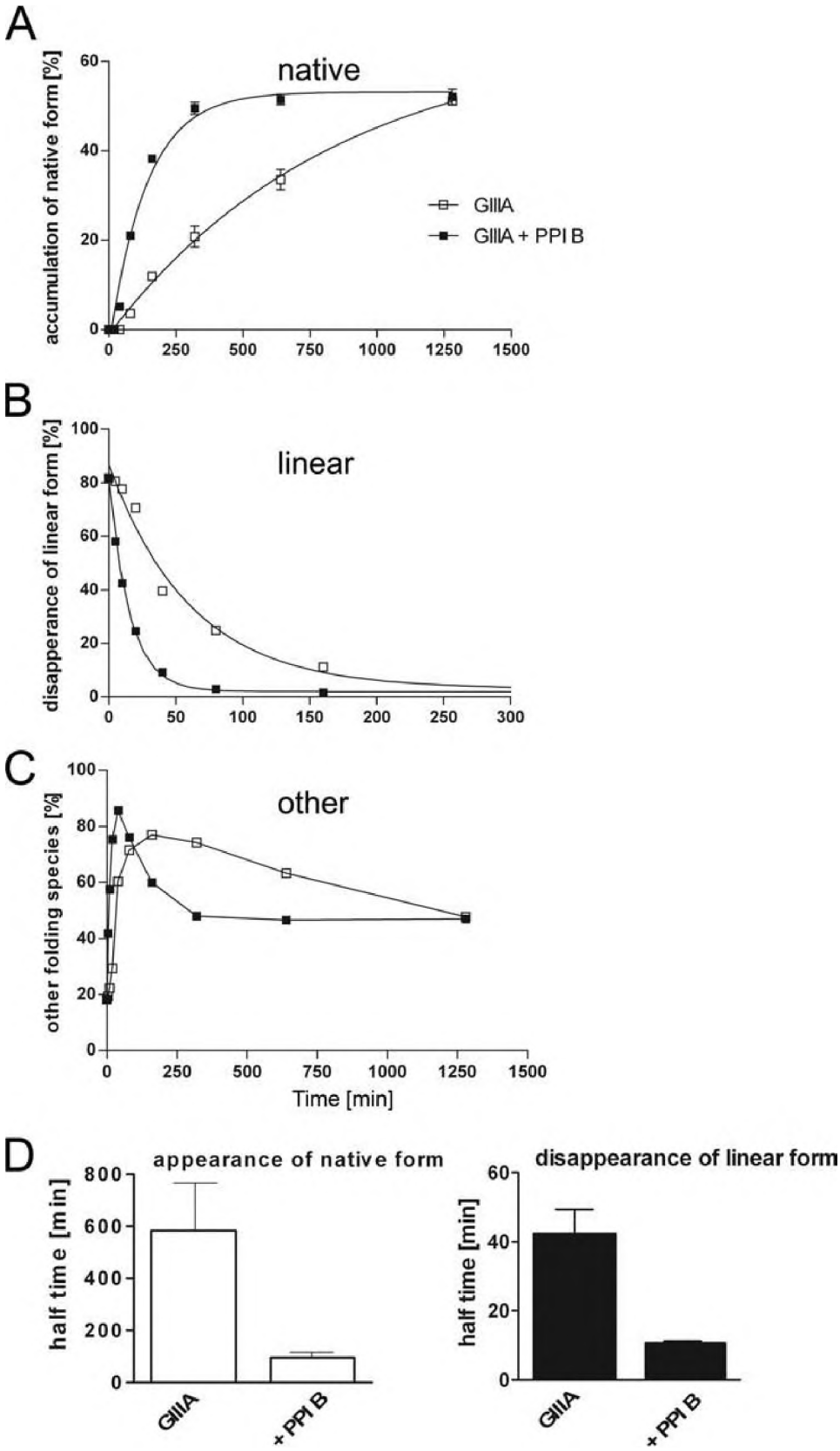

FIGURE 8. **Folding kinetics of μ-GIIIA in the presence of 0.1 mM GSH and 0.1 mM GSSG with and without *Conus* PPI B.** The relative abundance of the correctly folded (*A*), linear (*B*), and other folding species (*C*) was determined by HPLC as shown in Fig. 7. The plotted values are averages from three independent experiments. Nonlinear regression analysis was performed on plotted data, and half-times for the appearance and disappearance were calculated for the native and linear forms, respectively (*D*).

shown for a number of proline-containing proteins including ribonuclease T1, PPIase can improve the efficiency of PDI-mediated folding by providing partially folded protein chains with the correct proline isomers (56). As folding intermediates are highly susceptible to degradation, accelerating the time needed from translation at the ribosome to generation of the protein in its final three-dimensional structure is energetically advantageous. The epithelial cells of the venom gland are highly specialized in peptide biosynthesis and secretion and energetically rely upon fast turnover rates.

Here, we have shown that *Conus* PPIases can significantly accelerate the formation of the native disulfide bonds for conotoxin μ-GIIIA, revealing that peptidylprolyl isomerization is a rate-limiting step in the oxidative folding of this conotoxin. The native peptide containing three disulfide bonds appeared ~6 times faster in the presence of PPI B. Concomitantly, both the disappearance of the linear form and the appearance and subsequent disappearance of other folding species were accelerated when *Conus* PPI B was added to the folding reaction (Figs. 7 and 8). Changes in the folding kinetics followed in a concentration-dependent manner with 10-fold higher folding rates for GIIIA in the presence of 2.5 μM PPI B (Fig. 9). No difference in GIIIA folding was observed when heat-treated enzyme was added to the folding reaction (data not shown).

As all three prolines in μ-GIIIA are posttranslationally modified, we have further demonstrated that a 4-hydroxyproline-containing conotoxin can be recognized by *Conus* PPIase, a finding reported previously for collagen (19, 20). Hydroxylation of prolines is believed to be catalyzed by prolyl 4-hydroxylase. Interestingly, PDI is a subunit of prolyl 4-hydroxylase, and hydroxylation, formation of the native disulfide bonds, and cis-trans isomerization of Hyp residues may occur concurrently. Recently a complex

TABLE 3

Half-times for the appearance of μ-GIIIA containing native disulfide connectivity in the presence of *Conus* PPIases

Half-times were calculatd by non-linear regression. The numbers in parentheses represent the upper and lower 95% confidence interval.

Enzyme	Half-time for appearance of native form
μM	min
No enzyme	583 (471–766)
PPI B, 0.025	275 (190–495)
PPI B, 0.1	181 (140–257)
PPI B, 0.5	100 (77–141)
PPI B, 2.5	61 (50–78)
PPI A (I), 2.5	220 (156–375)
PPI A (II), 2.5	244 (173–414)

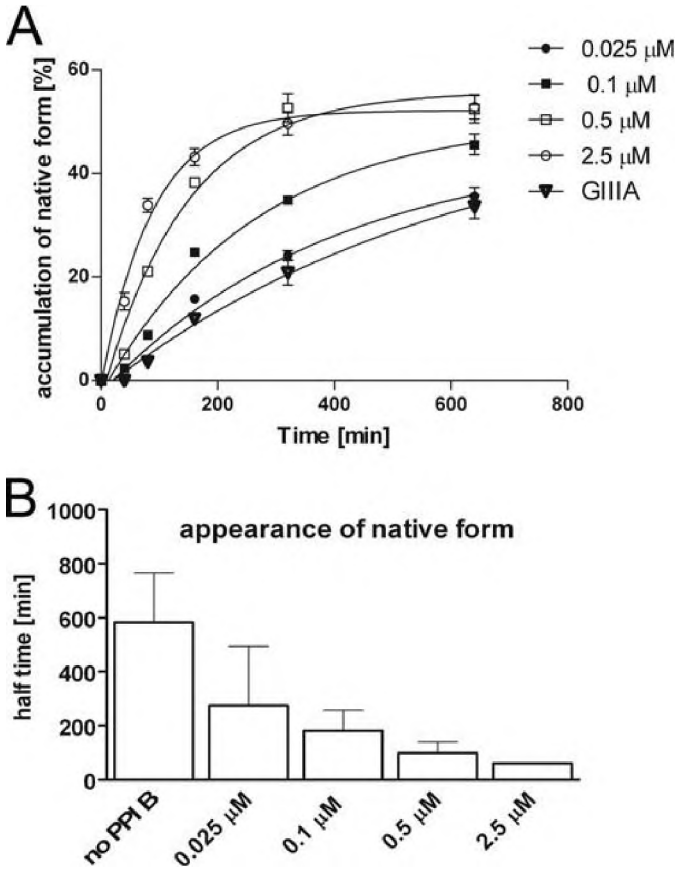

FIGURE 9. **Folding kinetics of μ-GIIIA in the presence of 0.1 mM GSH and 0.1 mM GSSG and different concentrations of *Conus* PPI B.** *A*, the plotted values are averages from three independent experiments. Nonlinear regression analysis was performed on the plotted data, and half-times were calculated for the appearance of the peptide containing the native disulfide connectivity (*B*).

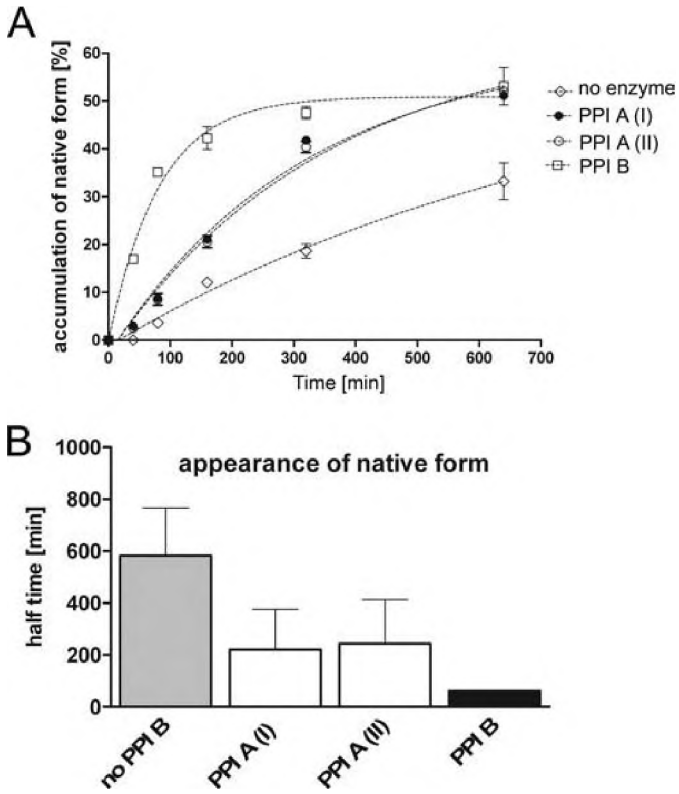

FIGURE 10. **Folding kinetics of μ-GIIIA in the presence of 0.1 mM GSH and 0.1 mM GSSG and different isoforms of *Conus* PPIase.** *A*, the effects of PPI A (I), PPI A (II), and PPI B on the oxidative folding of GIIIA were tested at a final concentration of 2.5 μM enzyme. The plotted values are averages from three independent experiments. Nonlinear regression analysis was performed on the plotted data, and half-times were calculated for the appearance of the peptide containing the native disulfide connectivity (*B*).

comprising prolyl 3-hydroxylase-1, cartilage-associated protein (CRTAP), and cyclophilin B was identified in chick embryos and shown to act as a chaperone for collagen (60). Similar complexes might be present in the ER of *Conus*, and their discovery would contribute greatly to our knowledge of the biosynthesis of conotoxins and other disulfide-rich small peptides.

Mature GIIIA is 22 amino acids in length and contains three Hyp residues in position 6, 7, and 17 (Table 2). NMR studies on GIIIA and its paralogue, GIIIB, strongly suggest a trans configuration of Hyp^6 and Hyp^{17}, whereas Hyp^7 adopts a cis conformation (54, 55). Under unstrained conditions, *e.g.* during translation at the ribosomes, most prolyl peptide bonds adopt a trans configuration (61). Therefore, for proteins containing both cis and trans prolines, the folding kinetics are driven by the trans-to-cis isomerization, and the contribution of the trans prolines can be neglected (39). As a consequence, $cis\text{-}Pro^7$ is likely to dominate the folding kinetics of GIIIA. However, slow intermediate trans-to-cis isomerizations of Pro^6 and Pro^{17} during formation and/or reshuffling of disulfide bonds cannot be ruled out.

The presence of PPIase did not affect the folding kinetics of ω-MVIIC and μ-SIIIA under the various conditions tested. The inability of *Conus* PPIs to accelerate the folding of SIIIA is not surprising, as this peptide does not contain Pro or Hyp residues. MVIIC is a ω-conotoxin with one Pro/Hyp residue likely to be present as mixed cis/trans isomers (18). Isomerization of the Pro/Hyp residue might not represent a rate-limiting step in the oxidative folding of MVIIC. Alternatively, MVIIC may not represent a suitable substrate for *Conus* PPIases. Both MVIIC and GIIIA comprise three disulfide bonds, are similar in length, and have comparable charge states at pH 7.5 (pH +4.2 for GIIIA and +5.2 for MVIIC). Studies addressing the substrate specificities of the PPIases of the cyclophilin family reveal the broad specificities of these enzymes (62, 63). However, short tetrapeptides were the only substrates tested in these studies (62, 63), and differences in substrate recognition and affinity between GIIIA and MVIIC cannot be excluded, especially considering

the significant differences in their disulfide patterns and primary amino acid sequences (see Table 2). Future studies using a variety of conotoxins with sequence similarities to GIIIA and MVIIC will shed light on substrate specificities of *Conus* PPIases.

RT-PCR on the venom gland, bulb, and muscle tissue revealed high expression levels of the ER-resident isoform PPI B in the venom gland of *C. novaehollandiae* (Fig. 4). As opposed to the bulb and the muscle, the venom gland is highly specialized for toxin biosynthesis, and up-regulation of PPI B strongly indicates a predominant role of this isoform in protein/peptide folding as reported for the human ER-resident PPIases CypB and FKBP-13 (36, 37). Furthermore, we have shown that *Conus* PPI B is approximately five times more efficient in accelerating the folding of GIIIA than the two cytosolic isoforms, PPI A (I) and A (II) (Fig. 10), but is less active in catalyzing the isomerization of the tetrapeptide Suc-AAPF-*p*NA (Fig. 6). These findings indicate a potential and specialized role of PPI B in the *in vivo* folding of conotoxins. Differences in catalytic efficacy between the A and B isoform have previously been reported for the trematode *Schistosoma mansoni* (64) and recently for human cyclophilins (65). Human CypA and CypB both recognize several proline residues on domain 2 of hepatitis C virus NS5A protein but with different catalytic efficiencies (65). For *S. mansoni* recombinant CypB was two to three times more active than CypA when tested against Suc-AAPF-*p*NA. As for *Conus* PPI A (I + II) and B, the amino acid residues important for substrate binding were highly conserved between the two isoforms with the only difference being the presence of serine 103 in PPIase B instead of the conserved alanine 103 for the A isoform. Although the authors (64) suggested that this amino acid replacement might cause the differences in substrate binding affinities, later studies demonstrated that the cytosolic A isoform can adopt two redox states, significantly impairing the enzyme activity (66). Under oxidizing conditions *S. mansoni* PPI A exhibits one disulfide bond, leading to a significant change in the binding pocket of the enzyme, thus impeding activity. A similar observation was made for cyclophilin CYP20–3 isolated from the chloroplasts of *Arabidopsis thaliana* (67, 68). CYP20-3, believed to be regulated by thioredoxin (68), comprises two disulfide bonds in its oxidized, inactive state (67). *Conus* PPI A (I) and (II) contain four cysteines in their primary amino acid sequence (Fig. 2). Formation of disulfide bonds between these cysteine residues may occur especially under the oxidizing conditions necessary for the conotoxin folding experiments. Only one cysteine remains conserved in the ER-resident *Conus* PPIase (Fig. 2), implying a potential adaptation of this isoform to the oxidizing conditions in the ER. Structural studies on the different PPIase isoforms under oxidizing and reducing conditions and in complex with Suc-AAPF-*p*NA, μ-GIIIA, and other potential conotoxin substrates will provide insight into the existence of redox states, differences in enzyme activities, and substrate recognition properties.

In summary, this study has identified the first members of the PPIase family in marine cone snails, animals that specialize in the biosynthesis of cysteine-rich peptides. We have demonstrated that a venom gland ER-resident isoform preferentially catalyzes the refolding of a conotoxin that contains three hydroxyprolines. These observations suggest that this isoform may have co-evolved with the toxin arsenal to efficiently produce the diverse venom repertoire of the *Conus* species. It is anticipated that *Conus* PPIases may act in concert with other foldases, such as PDI and prolyl 4-hydroxylase, to facilitate conotoxin biosynthesis. The characterization of these enzymes provides insights into the fundamental process of the folding of toxins and related polypeptides as well as having potential industrial application to the large scale production of toxins as therapeutics.

Acknowledgments—We thank Dr. Bruce Livett for his support and for comments on the manuscript, Bruce Abaloz for help with histological preparations, Dr. Robyn Bradbury and John Ahern for specimen maintenance, Dr. Konkallu Hanumae Gowd for help with folding studies, and Dr. Neil Young for help with histology and figures and for insightful discussions.

REFERENCES

1. Olivera, B. M. (1997) *Mol. Biol. Cell* **8,** 2101–2109
2. Terlau, H., and Olivera, B. M. (2004) *Physiol. Rev.* **84,** 41–68
3. Olivera, B. M. (2006) *J. Biol. Chem.* **281,** 31173–31177
4. Buczek, O., Bulaj, G., and Olivera, B. M. (2005) *Cell. Mol. Life Sci.* **62,** 3067–3079
5. Craig, A. G., Park, M., Fischer, W. H., Kang, J., Compain, P., and Piller, F. (2001) *Toxicon* **39,** 809–815
6. Loughnan, M. L., Nicke, A., Jones, A., Adams, D. J., Alewood, P. F., and Lewis, R. J. (2004) *J. Med. Chem.* **47,** 1234–1241
7. Mann, M., and Jensen, O. N. (2003) *Nat. Biotechnol.* **21,** 255–261
8. Pisarewicz, K., Mora, D., Pflueger, F. C., Fields, G. B., and Marí, F. (2005) *J. Am. Chem. Soc.* **127,** 6207–6215
9. Buczek, O., Yoshikami, D., Bulaj, G., Jimenez, E. C., and Olivera, B. M. (2005) *J. Biol. Chem.* **6,** 4247–4253
10. Bulaj, G., and Olivera, B. M. (2008) *Antioxid. Redox Signal.* **10,** 141–155
11. Bulaj, G., Zhang, M. M., Green, B. R., Fiedler, B., Layer, R. T., Wei, S., Nielsen, J. S., Low, S. J., Klein, B. D., Wagstaff, J. D., Chicoine, L., Harty, T. P., Terlau, H., Yoshikami, D., and Olivera, B. M. (2006) *Biochemistry* **45,** 7404–7414
12. De La Cruz, R., Whitby, F. G., Buczek, O., and Bulaj, G. (2003) *J. Pept. Res.* **61,** 202–212
13. Wang, Z. Q., Han, Y. H., Shao, X. X., Chi, C. W., and Guo, Z. Y. (2007) *FEBS J.* **274,** 4778–4787
14. Bulaj, G., Buczek, O., Goodsell, L., Jimenez, E. C., Kranski, J., Nielsen, J. S., Garrett, J. E., and Olivera, B. M. (2003) *Proc. Natl. Acad. Sci. U. S. A.* **100,** 14562–14568
15. Gowd, K. H., Krishnan, K. S., and Balaram, P. I. (2007) *Mol. Biosyst.* **3,** 554–566
16. Armishaw, C., Jensen, A. A., Balle, T., Clark, R. J., Harpsøe, K., Skonberg, C., Liljefors, T., and Strømgaard, K. (2009) *J. Biol. Chem.* **284,** 9498–9512
17. Townsend, A., Livett, B. G., Bingham, J.-P., Truong, H. T., Karas, J. A., O'Donnell, P., Williamson, N. A., Purcell, A. W., and Scanlon, D. (2009) *Int. J. Pept. Res. Ther.* **15,** 195–203
18. Lopez-Vera, E., Walewska, A., Skalicky, J. J., Olivera, B. M., and Bulaj, G. (2008) *Biochemistry* **47,** 1741–1751
19. Steinmann, B., Bruckner, P., and Superti-Furga, A. (1991) *J. Biol. Chem.* **266,** 1299–1303
20. Bächinger, H. P. (1987) *J. Biol. Chem.* **262,** 17144–17148
21. Davis, J. M., Boswell, B. A., and Bächinger, H. P. (1989) *J. Biol. Chem.* **264,** 8956–8962
22. Galat, A. (2003) *Curr. Top. Med. Chem.* **3,** 1313–1347
23. Arevalo-Rodriguez, M., Wu, X., Hanes, S. D., and Heitman, J. (2004) *Front. Biosci.* **9,** 2420–2446
24. Dolinski, K., Muir, S., Cardenas, M., and Heitman, J. (1997) *Proc. Natl.*

Acad. Sci. U. S. A. **94,** 13093–13098
25. Brazin, K. N., Mallis, R. J., Fulton, D. B., and Andreotti, A. H. (2002) *Proc. Natl. Acad. Sci. U. S. A.* **99,** 1899–1904
26. Rycyzyn, M. A., and Clevenger, C. V. (2002) *Proc. Natl. Acad. Sci. U. S. A.* **99,** 6790–6795
27. Yang, W. M., Inouye, C. J., and Seto, E. (1995) *J. Biol. Chem.* **270,** 15187–15193
28. Luban, J., Bossolt, K. L., Franke, E. K., Kalpana, G. V., and Goff, S. P. (1993) *Cell* **73,** 1067–1078
29. Bosco, D. A., Eisenmesser, E. Z., Pochapsky, S., Sundquist, W. I., and Kern, D. (2002) *Proc. Natl. Acad. Sci. U. S. A.* **99,** 5247–5252
30. Stamnes, M. A., Shieh, B. H., Chuman, L., Harris, G. L., and Zuker, C. S. (1991) *Cell* **65,** 219–227
31. Handschumacher, R. E., Harding, M. W., Rice, J., Drugge, R. J., and Speicher, D. W. (1984) *Science* **226,** 544–547
32. Liu, J., Farmer, J. D., Jr., Lane, W. S., Friedman, J., Weissman, I., and Schreiber, S. L. (1991) *Cell* **66,** 807–815
33. O'Keefe, S. J., Tamura, J., Kincaid, R. L., Tocci, M. J., and O'Neill, E. A. (1992) *Nature* **357,** 692–694
34. Price, E. R., Zydowsky, L. D., Jin, M. J., Baker, C. H., McKeon, F. D., and Walsh, C. T. (1991) *Proc. Natl. Acad. Sci. U. S. A.* **88,** 1903–1907
35. Nigam, S. K., Jin, Y. J., Jin, M. J., Bush, K. T., Bierer, B. E., and Burakoff, S. J. (1993) *Biochem. J.* **294,** 511–515
36. Kim, J., Choi, T. G., Ding, Y., Kim, Y., Ha, K. S., Lee, K. H., Kang, I., Ha, J., Kaufman, R. J., Lee, J., Choe, W., and Kim, S. S. (2008) *J. Cell Sci.* **121,** 3636–3648
37. Bush, K. T., Hendrickson, B. A., and Nigam, S. K. (1994) *Biochem. J.* **303,** 705–708
38. Rassow, J., Mohrs, K., Koidl, S., Barthelmess, I. B., Pfanner, N., and Tropschug, M. (1995) *Mol. Cell Biol.* **15,** 2654–2662
39. Schindler, T., Mayr, L. M., Landt, O., Hahn, U., and Schmid, F. X. (1996) *Eur. J. Biochem.* **241,** 516–524
40. di Luccio, E., Azulay, D. O., Fajloun, Z., Sandoz, G., Mansuelle, P., Kharrat, R., Fathallah, M., Carrega, L., Estève, E., Rochat, H., De Waard, M., and Sabatier, J. M. (2001) *Biochem. J.* **358,** 681–692
41. Pantin, C. F. A. (1946) *Notes on Microscopical Technique for Zoologists*, p. 75, Cambridge University Press, Cambridge
42. Shevchenko, A., Tomas, H., Havlis, J., Olsen, J. V., and Mann, M. (2006) *Nat. Protoc.* **1,** 2856–2860
43. Katoh, K., Kuma, K., Toh, H., and Miyata, T. (2005) *Nucleic Acids Res.* **20,** 511–518
44. Emanuelsson, O., Brunak, S., von Heijne, G., and Nielsen, H. (2007) *Nat. Protoc.* **2,** 953–971
45. Pace, C. N., Vajdos, F., Fee, L., Grimsley, G., and Gray, T. (1995) *Protein Sci.* **4,** 2411–2423
46. Fischer, G., Bang, H., and Mech, C. (1984) *Biomed. Biochim. Acta* **43,** 1101–1111
47. Fuller, E., Green, B. R., Catlin, P., Buczek, O., Nielsen, J. S., Olivera, B. M., and Bulaj, G. (2005) *FEBS J.* **272,** 1727–1738
48. Atherton, E., and Sheppard, R. C. (1989) *Solid Phase Peptide Synthesis: A Practical Approach*, pp. 134–139, University Press, Oxford, UK
49. Göthel, S. F., and Marahiel, M. A. (1999) *Cell. Mol. Life Sci.* **55,** 423–436
50. Kallen, J., Spitzfaden, C., Zurini, M. G., Wider, G., Widmer, H., Wüthrich, K., and Walkinshaw, M. D. (1991) *Nature* **353,** 276–279
51. Ke, H. M., Zydowsky, L. D., Liu, J., and Walsh, C. T. (1991) *Proc. Natl. Acad. Sci. U. S. A.* **88,** 9483–9487
52. Le Gall, F., Favreau, P., Richard, G., Letourneux, Y., and Molgó, J. (1999) *Toxicon* **37,** 985–998
53. Walewska, A., Zhang, M. M., Skalicky, J. J., Yoshikami, D., Olivera, B. M., and Bulaj, G. (2009) *Angew. Chem. Int. Ed. Engl.* **48,** 2221–2224
54. Hill, J. M., Alewood, P. F., and Craik, D. J. (1996) *Biochemistry* **35,** 8824–8835
55. Lancelin, J. M., Kohda, D., Tate, S., Yanagawa, Y., Abe, T., Satake, M., and Inagaki, F. (1991) *Biochemistry* **30,** 6908–6916
56. Schönbrunner, E. R., and Schmid, F. X. (1992) *Proc. Natl. Acad. Sci. U. S. A.* **89,** 4510–4513
57. Jakubowski, J. A., Kelley, W. P., and Sweedler, J. V. (2006) *Toxicon* **47,** 688–699
58. Stanley, T. B., Stafford, D. W., Olivera, B. M., and Bandyopadhyay, P. K. (1997) *FEBS Lett.* **407,** 85–88
59. Buczek, O., Olivera, B. M., and Bulaj, G. (2004) *Biochemistry* **43,** 1093–1101
60. Ishikawa, Y., Wirz, J., Vranka, J. A., Nagata, K., and Bächinger, H. P. (2009) *J. Biol. Chem.* **284,** 17641–17647
61. Balbach, J., and Schmid, F. X. (2000) in *Mechanisms of Protein Folding* (Pain, R. H., ed) pp. 212–249, Oxford University Press, Oxford, UK
62. Harrison, R. K., and Stein, R. L. (1990) *Biochemistry* **29,** 3813–3816
63. Harrison, R. K., and Stein, R. L. (1992) *J. Am. Chem. Soc.* **114,** 3464–3471
64. Bugli, F., Khattab, A., Vigneti, E., Butler, R., Cioli, D., and Klinkert, M. Q. (1998) *Protein Expr. Purif* **12,** 340–346
65. Hanoulle, X., Badillo, A., Wieruszeski, J. M., Verdegem, D., Landrieu, I., Bartenschlager, R., Penin, F., and Lippens, G. (2009) *J. Biol. Chem.* **284,** 13589–13601
66. Gourlay, L. J., Angelucci, F., Baiocco, P., Boumis, G., Brunori, M., Bellelli, A., and Miele, A. E. (2007) *J. Biol. Chem.* **282,** 24851–24857
67. Laxa, M., König, J., Dietz, K. J., and Kandlbinder, A. (2007) *Biochem. J.* **401,** 287–297
68. Motohashi, K., Koyama, F., Nakanishi, Y., Ueoka-Nakanishi, H., and Hisabori, T. (2003) *J. Biol. Chem.* **34,** 31848–31852